Adapting particle methods to model the dynamics of concentration gradients and chemical reactivity under advective diffusive transport conditions

A. Beaudoin[1], J.R. de Dreuzy and S. Huberson.

[1]Institute Pprime, Téléport 2, Boulevard Marie et Pierre Curie, BP 30179, 86962 Futuroscope Chasseneuil Cedex France.

Abstract

Concentration organization and dynamics in heterogeneous porous media are key physical factors driving chemical reactivity. At equilibrium, reactivity depends not only on the concentration distribution but also on concentration gradients. As high and low values of concentration and concentration gradient do not superpose, we derive a transport equation for the concentration gradients and set up an adapted particle method to approach them numerically. Particles dynamically optimize their organization to provide highly accurate concentration gradients. The global strategy combining separate particle methods for the concentration and its gradient gives optimal predictions of reactivity.

Keywords: *transport equation concentration gradient particle methods diffusion velocity method.*

1 Introduction

Particle methods are frequently used to model transport processes in porous and fractured media [6] [13] [21] [30]. When transport by advection largely dominates dispersion and diffusion processes, particle methods offer a relevant alternative to Eulerian methods [23] [72] [74]. Even though recent developments in Eulerian methods have reduced numerical diffusion issues [40] [58], particle methods remain broadly appropriate to low dispersion conditions [18] [59]. Particles efficiently adapt to flow structures and to local diffusive and dispersive conditions [8] [49] [68] [69]. They can integrate exchanges between high and low flow zones with potentially sharp interfaces (e.g. fracture/matrice) [54] [55] as well as chemical interactions with minerals and biofilms [5] [33] [64] [65]. Because particles naturally resolve the multi-scale diversity of the transport conditions, they are frequently used to model flows with slight density variations processes that emerge from their collective behavior. It is the case of the upscaled dispersion also called macro-dispersion that results from the differential influence of deterministic velocity correlations and stochastic dispersive/diffusive processes [7] [20] [66].

Particle methods become more involved when the process of interest is driven by local interactions between particles as it is typically the case for reactions between solute species (homogeneous reactions). As reactivity is often nonlinearly sensitive to solute concentrations [3], particle methods have progressively evolved from random walk methods where independent particles are tracked following a Fokker-Planck equation [35] [52] [68] to meshfree methods with interacting particles carrying concentration properties [6] [30] [65]. Such methods provide continuous estimates of the concentration field that can be coupled numerically to chemical reactivity like any other Eulerian transport method [19] [62] [71]. Particle methods are relevant to model the chemical control of reactivity expressed in terms of concentrations but not the physical control expressed in terms of concentration gradients [23] [57]. In fact, reactivity is physically controlled by the diffusive mixing of solutes of different chemical concentrations, as mixing two waters with equilibrated solute concentrations generally results in an out-of-equilibrium solution [41] [60] [61]. High concentration gradients thus promote diffusion, mixing and reactivity.

Particle methods are optimized to model concentration fields and not concentration gradients [23] [57]. Whether independent or interacting, particles become sparser in the medium because of spreading and dilution following the overall decrease of concentrations. Particles move apart and, after some time, can no longer resolve the spatial variations of the velocity field, challenging any approximation of concentration gradients. While particle reseeding is commonly used for concentrations [6] [13] [21] [30], we propose here a complementary strategy based on solving directly for concentration gradients instead of deriving concentra-

tion gradients from any approximation of the concentration field. Similar approaches have been studied for convective flows of slightly varying density [1].

We focus here on advection-diffusion processes in hetegeneous porous media. From the transport equation of concentrations, we derive the transport equation of concentration gradients and show how both differ (section 2). We propose adapted particle methods to solve the concentration gradients (section 3). we finally show how these methods, the particle method for the concentration (CPM) and the particle method for the concentration gradient (GPM), can be combined to compute reactivity rates when controlled both by concentrations and concentration gradients (section 5).

2 Transport equation of the concentration gradient

We focus here on advective and diffusive processes common in the transport of contaminants in porous media [4] [44]. In order to derive the transport equation of the concentration gradient, the gradient operator ∇ is applied to the advection - diffusion equation:

$$\nabla\left(\frac{\partial c}{\partial t} - \nabla\cdot(D\mathbf{g}) + \nabla\cdot(\mathbf{u}c)\right) = 0 \quad \text{with} \quad \mathbf{g} = \nabla c. \tag{1}$$

c is the concentration $[ML^{-3}]$, D is the diffusion coefficient $[L^2T^{-1}]$, $\mathbf{g}$ is the concentration gradient $[ML^{-4}]$ and $\mathbf{u}$ is the flow velocity $[LT^{-1}]$. As $\nabla \wedge \mathbf{g}$ is zero and D is constant, the second term of equation (1) is given by:

$$\nabla(\nabla\cdot(D\mathbf{g})) = \nabla\cdot(\nabla(D\mathbf{g})) + \nabla\wedge(\nabla\wedge(D\mathbf{g})) = \nabla\cdot(\nabla(D\mathbf{g})). \tag{2}$$

Water flow being incompressible and irrotational in porous media, the third term of equation (1) is given by:

$$\begin{aligned}\nabla(\nabla\cdot(\mathbf{u}c)) &= \nabla((\nabla c)\cdot\mathbf{u}) + (\nabla\cdot\mathbf{u})c) \\ &= (\mathbf{u}\cdot\nabla)\mathbf{g} + (\mathbf{g}\cdot\nabla)\mathbf{u} \\ &= \nabla\cdot(\mathbf{u}\otimes\mathbf{g}) + (\mathbf{g}\cdot\nabla)\mathbf{u}\end{aligned} \tag{3}$$

where $\otimes$ is the tensorial product. The substitution of the two simplifications (Eq. 2) and (Eq. 3) in equation (1) yields:

$$\frac{\partial \mathbf{g}}{\partial t} - \nabla\cdot(\nabla(D\mathbf{g})) + \nabla\cdot(\mathbf{u}\otimes\mathbf{g}) + (\mathbf{g}\cdot\nabla)\mathbf{u} = 0. \tag{4}$$

The second term of the previous equation describes the diffusion of the concentration gradient and the last two terms represent the transport of the concentration gradient by the velocity field. Three distinct effects are included. The first is the displacement of the gradient application point by the local velocity. This local velocity also induces a displacement and a distorsion of concentration iso-contours. The variation of the distance between two such lines results in variations of the gradient intensity. These two effects are accounted for by the last term of equation (4). The last step consists in writing the diffusive term of equation (4) as an advective term by means of a diffusion velocity method [6] [8] [47] [48] [50]:

$$\frac{\partial \mathbf{g}}{\partial t} + \nabla\cdot((\mathbf{u_d}+\mathbf{u})\otimes\mathbf{g}) + (\mathbf{g}\cdot\nabla)\mathbf{u} = 0 \tag{5}$$

where $\mathbf{u_d}$ is the diffusion velocity $[LT^{-1}]$. The transport equation of the concentration gradient (Eq. 4) is then transformed in a purely advection equation with a source term (Eq. 5). Particle methods are well suited to solve the pure advection equation [14] [38] [11]. It must be noticed that the gradient vector $\mathbf{g}$ is not affected by this transformation. Actually, the effect of the diffusion is to move the concentration iso-contours. The advection term is thus modified in order to transport the gradient application point accordingly. This operation ensures the consistency between the concentration and its gradient at any point. The expression of $\mathbf{u_d}$ is derived by means of a simple identification between equations (4) and (5):

$$\mathbf{u_d}\otimes\mathbf{g} = -\nabla(D\mathbf{g}). \tag{6}$$

It must be pointed out that the Particle Strength Exchange method can be considered as a valuable alternative to the Velocity Diffusion Method [17]. Both approaches have their advantages and drawbacks [74] [6]. In our case, the main advantages of the velocity diffusion method is the straightforward inclusion of the heterogeneity of porous media in the formulation and the ability of the method to account for unbounded flows without any additional equation. Respective avantages of both method should be further discussed for

selecting optimal strategies. Although the Diffusion Velocity Method was introduced more than thirty years ago, there are still only few mathematical studies available [12]. In [43], the convergence of the method was shown for the case of the linear heat equation. Therefore, in the absence of any other theoretical work, the problem arising when the Hessian is zero has been assumed to be a numerical difficulty for which different solutions can be applied (see for example [63]). Here, the simplest method was used by imposing a lower bound to the Hessian.

3 Particle method for solving the concentration gradient equation

In this section, we develop a particle method to solve the transport equation for the concentration gradient (Eq. 5). We show how the diffusion velocity is estimated, and how concentrations are derived from concentration gradients.

3.1 Particles carrying the concentration gradient

We build up an initial set of particles carrying the concentration gradient on the basis of a regular grid to define the initial values of the components of $\mathbf{g}$ [14] [38]. Each particle $\mathcal{P}_i$ is defined by its location $\mathbf{x}_i$ $[L]$ corresponding to the center of one grid cell and its gradient vector $\mathbf{g}_i$ $[ML^{-2}]$ in which each component corresponds to its quantity contained in the grid cell:

$$\mathbf{g_i} = \int_{|\mathcal{P}_i|} \mathbf{g}(\mathbf{x}')d\mathbf{x}' \approx \mathbf{g}(\mathbf{x_i})|\mathcal{P}_i| \tag{7}$$

where $|\mathcal{P}_i|$ is the support of the particle $\mathcal{P}_i$ $[L^2]$. When a regularly spaced cartesian grid is used, the result is a set of equidistant particles with different weights according to their location on the grid. The concentration gradient can be approximated by:

$$\mathbf{g}_h = \sum_i \mathbf{g_i}\zeta_\epsilon\left(\mathbf{x} - \mathbf{x}_i\right) \quad \text{with} \quad \zeta_\epsilon(\mathbf{x}) = (1/\epsilon^d)\zeta(\mathbf{x}/\epsilon) \tag{8}$$

where $\mathbf{g}_h$ is the approximated concentration gradient, ζ_ϵ is a smoothing function and d is the Euclidean dimension of the problem. In this work, a 2D Gaussian smoothing function was selected for the two-dimensional examples later shown:

$$\zeta_\epsilon(\mathbf{x}) = \frac{1}{\pi\epsilon^2}\exp\left(-\frac{|\,\mathbf{x}\,|^2}{\epsilon^2}\right). \tag{9}$$

The smoothing parameter ϵ $[L]$ is proportional to the grid cell size h $[L]$ used to generate the particles, ϵ/h is held constant [6] [14] [74]. To solve the transport equation for the concentration gradient (Eq. 5), it is written in a Lagrangian framework yielding the discrete form:

$$\frac{d\mathbf{x}_i}{dt} = \mathbf{u}(\mathbf{x}_i) + \mathbf{u_d}(\mathbf{x}_i) \quad \text{and} \quad \frac{d\mathbf{g}_i}{dt} = -\mathbf{g}_i\nabla\mathbf{u}(\mathbf{x}_i). \tag{10}$$

This set of differential equations is numerically solved by using a 4th order accurate Runge - Kutta scheme [6] [45] [74]. The time step δt is fixed according to the CFL conditions $\delta t = \min(h/|\mathbf{u}|, \sqrt{h^2/D})$ $[T]$ [6] [46] [74]. This condition is probably not optimal since it has been shown, at least for the case of a linear convection equation, that a so-called "Lagrangian CFL condition" should be a better choice [15]. However, the former condition, although somewhat conservative, was prefered in our work because of the presence of an additional diffusion term. Subjected to the effects of flow and diffusion velocities, the set of particles becomes progressively non uniform. In order to maintain the overlap relation ϵ/h = constant, a classical regridding process is used here all the $N_{\delta t}$ time steps [6] [14] [74].

3.2 Estimation of the diffusion velocity

To express the diffusion velocity $\mathbf{u_d}$, the divergence operator $\nabla\cdot$ is applied to equation (6):

$$\nabla\cdot(\mathbf{u_d}\otimes\mathbf{g}) = -\nabla\cdot(\nabla(D\mathbf{g})). \tag{11}$$

As the diffusion coefficient D is constant, the right hand side reads:

$$\nabla\cdot(\mathbf{u_d}\otimes\mathbf{g}) = -D\Delta\mathbf{g}. \tag{12}$$

From the definition of the tensorial product, the previous equation can be rewritten by:

$$(\mathbf{u_d} \cdot \nabla)\mathbf{g} = -D\Delta\mathbf{g}. \tag{13}$$

The components of the diffusion velocity $\mathbf{u_d}$ are determined by solving the system of equations (13) by means of Cramer's rule [9]:

$$\begin{cases} u_{dx} = -D\left(\Delta g_x \frac{\partial g_y}{\partial y} - \Delta g_y \frac{\partial g_x}{\partial y}\right) / \left(\frac{\partial g_x}{\partial x}\frac{\partial g_y}{\partial y} - \frac{\partial g_x}{\partial y}\frac{\partial g_y}{\partial x}\right) \\ u_{dy} = -D\left(\Delta g_y \frac{\partial g_x}{\partial x} - \Delta g_x \frac{\partial g_y}{\partial x}\right) / \left(\frac{\partial g_x}{\partial x}\frac{\partial g_y}{\partial y} - \frac{\partial g_x}{\partial y}\frac{\partial g_y}{\partial x}\right) \end{cases} \tag{14}$$

where (u_{dx},u_{dy}) and (g_x,g_y) are respectively the components of the diffusion velocity $\mathbf{u_d}$ and of the concentration gradient $\mathbf{g}$.

3.3 Derivation of the concentration from its gradient

The computation of the concentration from particles carrying the concentration gradient $\mathbf{g}$ can not be performed by means of a direct convolution product because the relation between c and $\mathbf{g}$ is a first order partial differential equation. We derive the concentration by solving the Poisson equation giving the concentration c from its gradient $\mathbf{g}$ obtained from equation (1 - right):

$$\Delta c = \nabla \cdot \mathbf{g}. \tag{15}$$

An integral solution of which, for an unbounded domain with zero external conditions, reads:

$$c(\mathbf{x}) = \int_{\mathcal{R}^2} G(\mathbf{x},\mathbf{x}')\nabla \cdot \mathbf{g}(\mathbf{x}')d\mathbf{x}' \quad \text{with} \quad G(\mathbf{x}) = \frac{1}{2\pi}\log \mid \mathbf{x} \mid \quad \text{in 2D} \tag{16}$$

where G is the Green function of Poisson equation [29] [31]. In this paper, the boundary conditions for the concentration were either unbounded domain conditions or periodic conditions. The flow was actually bounded in two directions because of the use of a finite volume solver. The absence of boundaries was simulated by using a flow domain much larger than the domain occupied by the particles. The velocity diffusion method only requires the knowledge of the flow velocity and concentration within this last domain.

4 Concentration versus gradient particle methods to simulate reactive transport in heterogeneous porous media

We show how the two particle methods can be used to simulate reactive transport in heterogeneous porous media. We first describe the reactive transport model and the medium properties. We then compare the accuracy and convergence of the concentration (CPM) and gradient (GPM) particle methods. We eventually propose a more optimal combination of both particle methods to improve the estimate of reactivity.

4.1 Chemical reactivity rate

The simple case of a dissolution/precipitation reaction at equilibrium is considered here. The precipitate component P is in equilibrium with the solutes A and B of concentrations c_A and c_B ($A + B \Leftrightarrow P$) [3]. Assuming that P is in a pure phase, its activity is equal to one, while activities of solute species are equal to their concentrations. c_A and c_B are then related by:

$$c_A \cdot c_B = K \tag{17}$$

with K the equilibrium constant [ML^{-3}]. The reactive transport equation of each specy can be expressed generically for c (either c_A or c_B) as:

$$\frac{\partial c}{\partial t} - \nabla \cdot (D\nabla c) + \nabla \cdot (\mathbf{u}c) = r. \tag{18}$$

The reactivity rate r [$ML^{-3}T^{-1}$] is derived by combining the equilibrium equation (21) and the reactive transport equations (22) for c_A and c_B:

$$r = \frac{2K}{((\delta c)^2 + K)^{3/2}}\nabla(\delta c)D\nabla(\delta c) \tag{19}$$

where $\delta c = c_A - c_B$ is the difference of concentrations between the species A and B [60]. δc is not modified by reactivity but only by transport processes. In fact, as δc is simply obtained by subtracting equations (22) expressed for each specy, it follows the classical transport equation:

$$\frac{\partial(\delta c)}{\partial t} - \nabla \cdot (D\nabla(\delta c)) + \nabla \cdot (\mathbf{u}(\delta c)) = 0. \tag{20}$$

The first term of the left-hand side of equation (23) comes from the chemical system. The second term shows that reactivity is physically induced by the local gradient of solute concentration imbalances [61]. This simple example shows how mixing and reactivity are activated by interactions between advective and dispersive processes traduced in the local-scale dynamics of concentration gradients [2] [42].

4.2 Benchmark description

The dissolution/precipitation reaction is modeled in a 2D heterogeneous porous medium defined by a rectangular domain of dimensions $L_x = 2048\ m$ and $L_y = 512\ m$ [7] [26] [66]. The porous medium is characterized by a random hydraulic conductivity field $K\ [LT^{-1}]$ following a stationary log-normal probability distribution, parametrized by a mean m and a Gaussian covariance function C given by [16] [25]:

$$C(\mathbf{r}) = \sigma^2 \exp\left(-\left(\frac{|\mathbf{r}|}{\lambda}\right)^2\right) \tag{21}$$

where $|\mathbf{r}|$ represents the separation distance between two points $[L]$. The mean m, the variance σ^2 and the correlation length λ are respectively equal to 0, 4 and 10 m. The generation of a correlated log-normal field is performed via a Fourier transform by means of the software FTTW [24] [28]. Steady state flows are described by mass conservation and Darcy's law [4] [44]:

$$\nabla \cdot \mathbf{u} = 0 \quad \text{and} \quad \mathbf{u} = -K\nabla\phi \tag{22}$$

where $\mathbf{u}$ and ϕ are the Darcean velocity $[LT^{-1}]$ and the hydraulic head $[L]$. The boundary conditions are permeameter-like with homogeneous Neumann on the upper and lower sides and Dirichlet $\phi = 0$ on the left side and $\phi = L_x$ on the right side. The flow equations are discretized on a regular grid using a Finite Volume scheme with the mesh resolution equal to 1 m in the two directions x and y [10] [53]. The resulting linear system is solved with the parallel algebraic multigrid method of HYPRE [22]. At initial time $t = 0\ h$, the difference of concentrations between the species A and B, δc_0, is injected at the point source $\mathbf{x_o} = (x_o = 256\ m,\ y_o = 256\ m)$. The set of particles is initialized by using the analytical solution of previous benchmark (Eq. 18 and 19) with $t = 0\ h$ and $\delta = 4\ h$. The re-griding frequency of particles $N_{\delta t}$ is fixed to 10 time steps for the two particle methods. The Peclet number is defined by $P_e = \lambda|\mathbf{u}_{mean}|/D$. The norm of the mean flow velocity $|\mathbf{u}_{mean}|$ is equal to 1 mh^{-1}. Thus the Peclet number P_e is equal to 100 for $D = 0.1\ m^2h^{-1}$.

4.3 Comparison of the two particle methods

On Fig. 8 (top), concentrations δc between the species A and B obtained by the concentration (CPM) and gradient (GPM) particle methods are broadly different. While δc obtained by CPM remains channelled along the velocity field as it should be [27] [34] [39] [67], GPM smoothes it critically because of the necessary integration between the concentration gradient and the concentration itself (Eq. 16). Smoothing effects accumulate with time eventually and remove the multiple concentration peaks at time $t = 150\ h$. This effect is especially marked in the red square zone indicated on Fig. 8.

Derivation of the two components g_x and g_y of the concentration gradient $\mathbf{g}$ from the concentration δc obtained with CPM induces oscillations like in the circular test case of section 4. These oscillations occur everywhere in the solute plume and are much stronger than in the circular test case likely because heterogeneity enhances concentration gradients.

Because each particle method gives accurate numerical results for each term of the reactivity rate r (Eq. 23), we propose a strategy combining CPM and GPM. The chemical term depending on δc is estimated by CPM. The physical term depending on $\nabla\delta c = \mathbf{g}$ is estimated by GPM. On Fig. 9, the reactivity rate r, obtained by this combination of particle methods, is presented at two times, $t = 75$ and $150\ h$, with a grid cell size $h = 0.64\ m$. No oscillation appears on the numerical results. Spatial variability of the velocity field broadly induces channeling and localised reactivity.

The convergence of the two particle methods proposed is assessed on the basis of the integral R of the

reactivity rate r over the computational domain:

$$R(t) = \int_{L_x \times L_y} r(\mathbf{x}, t) dxdy. \tag{23}$$

As shown on Fig. 10, the evolution of R with CPM is not monotonous and thus does not converge. The two other particle methods give results close and display monotonous trends. The combined particle method especially gives very consistent results for the three particle resolutions showing good convergence properties. It also shows that a limited number of particles gives acceptable approximations of reactivity.

In terms of performances, the particle number N_p increases with the same trend for the two particle methods, CPM and GPM, as the concentration plume spreads in the porous medium (see Fig. 11). As the spreading eventually scales in both directions with the square root of time, N_p scales linearly in the intermediary asymptotic regime. Table 1 gives the iteration number N_{iter}, the time step δt and the CPU time obtained by CPM and GPM for the three values of the grid cell size h tested here. As CPM and GPM give the same time evolution of N_p (see Fig. 11), the CPU times obtained by the two particle methods are very close. Then an optimal solution is the combination of the two particle methods with a grid cell size h = 1.28 m. This solution gives accurate predictions of reactivity with a reasonable CPU time.

5 Conclusions

Concentration gradients are generally estimated from concentrations on the basis of finite difference methods. This approach depends not only on the order of accuracy of finite differences but also on the order of the method used for estimating the concentration. In this work, solving directly the transport equation of concentration gradient has improved the description of concentration gradients. Obtaining this transport equation has revealed a stretching term that takes into account a vectorial adaptation of concentration gradients to the topology of iso-concentration lines. Meshfree particle methods inherently conserve this characteristic. While estimates of concentration gradients are accurate, reconstructed concentrations are too smooth as a result of the necessary integration. As reactivity eventually depends on the concentration and its gradient, we propose a global strategy combining separate particle methods for the concentration and its gradient. Prospective results show that this solution gives accurate predictions of reactivity. As the CPU time stays reasonable, the futur work is to use this solution for studying reactivity in higher heterogeneous porous media. The extension to 3-D cases will be also considered. It is straigthfoward and does not require any new development exepted drastic improvements in the computational efficiency of the code.

Acknowledgments

The French National Research Agency ANR is acknowledged for its financial founding through the H2MNO4 project (ANR - 12 - MONU - 0012).

References

[1] C.R. Anderson, A vortex method for flows with slight density variations, J. Comput. Phys., 61 (1985), 417-444.

[2] P. de Anna, M. Dentz, A. Tartakovsky and T. Le Borgne, The filamentary structure of mixing fronts and its control on reaction kinetics in porous media flows, Geophys. Res. Lett., 41 (2014) 4586-4593.

[3] C. Appelo and D. Postma, Geochemistry, Groundwater and Pollution, AA Balkema, Brookfield, 1994.

[4] J. Bear, Hydraulics of groundwater, McGraw-Hill, New York, 1979.

[5] K. Besnard, J.R. de Dreuzy, P. Davy and L. Aquilina, A modified Lagrangian-volumes method to simulate nonlinearly and kinetically sorbing solute transport in heterogeneous porous media, J. Contam. Hydrol., 120-121 (2011) 89-98.

[6] A. Beaudoin, S. Huberson and E. Rivoalen, Simulation of anisotropic diffusion by means of a diffusion velocity method, J. Comput. Phys., 186 (2003) 122-135.

[7] A. Beaudoin, J. Erhel and J.R. de Dreuzy, A comparison between a direct and a multigrid sparse linear solvers for highly heterogeneous flux computations, Eccomas CFD 2006, volume CD, 2006.

[8] A. Beaudoin, S. Huberson and E. Rivoalen, A particle method for solving Richard's equation, C.R. Acad. Sci., Ser. IIb: Mec., 339 (2011) 257-261.

[9] M. Brunetti, Old and new proofs of cramer's rule, Applied Mathematical Sciences, 8 (2014) 6689-6697.

[10] G. Chavent and J. E. Roberts, A unified physical presentation of mixed, mixed-hybrid finite elements and standard finite difference approximations for the determination of velocities in waterflow problems, Adv. Water Resour., 14 (1991) 329-348.

[11] A. Chertock and D. Levy, Particle methods for dispersive equations, J. Comput. Phys., 171 (2001) 708-730.

[12] J.P. Choquin and S. Huberson, Particle simulation of viscous flow, Comp. and fluids, 17 (1989), p 397.

[13] P.W. Cleary and J.J. Monaghan, Conduction modelling using smoothed particle hydrodynamics, J. Comput. Phys., 148 (1999) 227-264.

[14] G.H. Cottet and P.D. Koumoutsakos, Vortex Methods Theory and Practice, Cambridge University Press, Mars 2000.

[15] G.H. Cottet, J.M. Etancelin, F. Perignon and C. Picard, High order semi-Lagrangian particle methods for transport equations: numerical analysis and implementation issues, ESAIM: M2AN, 48 (2014), 1029-1060.

[16] G. Dagan, Solute transport in heterogeneous porous formation, J. Fluid Mech., 145 (1984) 151-177.

[17] P. Degond, S. Mas-Gallic, The weighted particle method for convection–diffusion equations, Part 2: The anisotropic case, Math. Comput., 53 (1989) 509.

[18] F. Delay, G. Porel and P. Sardini, Modelling diffusion in a heterogeneous rock matrix with a time-domain Lagrangian method and an inversion procedure, C.R. Acad. Sci., Ser. IIa: Sci. Terre Planets, 334 (2002) 967-973.

[19] C. de Dieuleveult, J. Erhel and M. Kern, A global strategy for solving reactive transport equations, J. Comput. Phys., 228 (2009) 6395-6410.

[20] J.R. de Dreuzy, A. Beaudoin and J. Erhel, Asymptotic dispersion in 2D heterogeneous porous media determined by parallel numerical simulations, Water Resour. Res., 43 (2007).

[21] S.M. Eberts, J.K. Bohlke, L.J. Kauffman and B.C. Jurgens, Comparison of particle-tracking and lumped-parameter age-distribution models for evaluating vulnerability of production wells to contamination, Hydrogeol. J., 20 (2012) 263-282.

[22] R.D. Falgout, J.E. Jones and U.M. Yang, Pursuing scalability for hypre's conceptual interfaces, ACM Trans. Math. Softw., 31 (2005) 326-350.

[23] D. Fernandez-Garcia and X. Sanchez-Vila, Optimal reconstruction of concentrations, gradients and reaction rates from particle distributions, J. Comput. Phys., 120-121 (2011) 99-114.

[24] M. Frigo and S.G. Johnson, The design and implementation of FFTW3, paper presented at the IEEE, 93 (Special Issue on Program Generation, Optimization, and Platform Adaptation), 2005.

[25] L. Gelhar and C. Axness, Three dimensional stochastic analysis of macrodispersion in aquifers, Water Resour. Res., 19 (1983) 161-180.

[26] L. Gelhar, Stochastic subsurface hydrology, Engelwood Cliffs, New Jersey, 1993.

[27] R. Le Goc, J.R. de Dreuzy and P. Davy, Statistical characteristics of flow as indicators of channeling in heterogeneous porous and fractured media, Advances in Water Resources, 33 (2010) 257-269.

[28] A.L. Gutjahr, Fast fourier transforms for random field generation, Project Report for Los Alamos Grant to New Mexico Tech, Contract number 4-R58-2690R, Department of Mathematics, New Mexico Tech, Socorro, New Mexico, 1989.

[29] M.J. Hancock, Method of Green's functions, Linear Partial Differential Equations, 2006

[30] P.A. Herrera, M. Massabo and R.D. Beckie, A meshless method to simulate solute transport in heterogeneous porous media, Adv. Water Resour., 32 (2009) 413-429.

[31] R. Hunt, Chapter 2 - Poissons Equation, Lecture Notes, University of Cambridge, 2007.

[32] M. Huysmans and A. Dassargues, Review of the use of Peclet numbers to determine the relative importance of advection and diffusion in low permeability environments, Hydrogeol. J., 2004.

[33] G.E. Kapellos, A.S. Terpsichori and A.C. Payatakes, Hierarchical simulator of biofilm growth and dynamics in granular porous materials, Adv. Water Resour., 30 (2007) 1648-1667.

[34] J. Kerrou, P. Renard, H.J. Hendricks Franssen and I. Lunati, Issues in characterizing heterogeneity and connvectivity in non-multiGaussian media, Adv. Water Resour., 31 (2008) 147-159.

[35] W. Kinzelbach, The random-walk method in pollutant transport simulation, Groundwater flow and quality modelling 1988, Springer, New York, NATO ASI Serie C, 227-245.

[36] L.F. Konikow, Applying dispersive changes to lagrangian particles in groundwater transport models, Transport Porous Med., 85 (2010) 437-449.

[37] L.F. Konikow, D.J. Goode and G.Z. Hornberger, A Three-dimensional method of characteristics solute-transport model (MOC3D), U.S. Geological Survey Water Resources Investigation Report, 96-4267, 1996.

[38] P. Koumoutsakos, Multiscale flow simulations using particles, Annu. Rev. Fluid Mech., 37 (2005) 457-487.

[39] C. Knudby and J. Carrera, On the relationship between indicators of geostatistical flow and transport connectivity, Adv. Water Resour., 28 (2005) 405-421.

[40] L.K. Lautz and D. I. Siegel, Modeling surface and ground water mixing in the hyporheic zone using MODFLOW and MT3D, Adv. Water Resour., 29 (2006) 1618-1633.

[41] T. Le Borgne, M. Dentz, D. Bolster, J. Carrera, J.R. de Dreuzy and P. Davy, Non-Fickian mixing : Temporal evolution of the scalar dissipation rate in heterogeneous porous media, Adv. Water Resour., 3 (2010) 1468-1475.

[42] T. Le Borgne, M. Dentz and E. Villermaux, Stretching, coalescence, and mixing in porous media, Phys. Rev. Lett., 110 (2013) 204501.

[43] P.L. Lions and S. Mas-Gallic, Une méthode particulaire déterministe pour des équations diffusives non linéaires, CRAS Sciences - Série I - Mathematica, 332 (2001), 369-376.

[44] G. de Marsily, Quantitative hydrogeology : groundwater hydrology for engineers, Academic press, Inc., San Diego, California, 1986.

[45] A. Mayer, Numerical approach of physical problems, Chapter 16 : Integration of ordinary differential equations, Lecture Notes, University of Namur, 2014.

[46] C.A. de Moura and C.S. Kubrusly, The Courant-Friedrichs-Lewy (CFL) Condition, Birkhauser, 2013.

[47] P. Mycek, G. Pinon, G. Germain and E. Rivoalen, Formulation and analysis of a diffusion-velocity particle model for transport-dispersion equations, Comput. Appl. Math., (2014) 1-27.

[48] P. Mycek, G. Pinon, G. Germain and E. Rivoalen, A self-regularising DVM-PSE method for the modelling of diffusion in particle methods, C.R. Acad. Sci., Ser. IIb: Mec., 341 (2013) 9-10.

[49] B. Noetinger, D. Roubinet, A. Russian, T. Leborgne, F. Delay, M. Dentz, J.R. de Dreuzy and P. Gouze, Random walk methods for modeling hydrodynamic transport in porous and fractured media from pore to reservoir scale, Transport Porous Med., (2016) 1-41.

[50] Y. Ogami and T. Akamatsu, Viscous flow simulation using the discrete vortex model - the diffusion velocity method, Comput. Fluids, 19 (1991) 433-444.

[51] D. Pokrajac and R. Lazic, An efficient algorithm for high accuracy particle trakcing in finite elements, Adv. Water Resour., 25 (2002) 353-369.

[52] M. Rahbaralam, D. Fernandez-Garcia and X. Sanchez-Vila, Do we really need a large number of particles to simulate bimolecular reactive transport with random walk methods ? A kernel density estimation approach, J. Comput. Phys., 303 (2015) 95-104.

[53] J.E. Roberts and J.M. Thomas, Mixed and hybrid methods, in Handbook of Numerical Analysis 2, Finite Element Methods part 1, edited by P.G. Ciarlet and J.L. Lions, 1991, 523-639, Elsevier Sci.

[54] D. Roubinet, H.H. Liu and J.R. de Dreuzy, A new particle-tracking approach to simulating transport in heterogeneous fractured porous media, Water Resour. Res., 46 (2010).

[55] D. Roubinet, J.R. de Dreuzy and D.M. Tartakovsky, Particle-tracking simulations of anomalous transport in hierarchically fractured rocks, Comput. Geosci., 50 (2013) 52-58.

[56] C.J. Roy and M.M. Hopkins, Discretization error estimates using exact solutions to nearby problems, IAA Paper 2003-0629.

[57] J. Rubin, Transport of reacting solutes in porous media - relation between mathematical nature of problem formulation and chemical nature of reactions, Water Resour. Res., 19 (1983) 1231-1252.

[58] T.F. Russell and M.A. Celia, (2002), An overview of research on Eulerian-Lagrangian localized adjoint methods (ELLAM), Adv. Water Resour., 25 (8-12) 1215-1231.

[59] P. Salamon, D. Fernandez-Garcia and J.J Gomez-Hernandez, A review and numerical assessment of the random walk particle tracking method, J. Contam. Hydrol., 87 (2006) 277-305.

[60] M. de Simoni, J. Carrera, X. Sanchez-Villa and A. Guadagnini, A procedure for the solution of multicomponent reactive transport problems, Water Resour. Res., 41 (2005).

[61] M. de Simoni, X. Sanchez-Vila, J. Carrera, M.W. Saaltink, A mixing ratios-based formulation for multicomponent reactive transport, Water Resour. Res., 43 (2007).

[62] C.I. Steefel, D.J. DePaolo and P.C. Luchtner, Reactive transport modeling : An essential tool and a new research approach for the Earth sciences, Earth Planet. Sci. Lett., 240 (2005) 539-558.

[63] J.H. Strickland, S.N. Kempka and W.P. Wolf, Viscous diffusion of vorticity in unsteady wall layers using the diffusion velocity concept, ESAIM Proceedings, 1 (1996), 13-151.

[64] N.Z. Sun, A finite cell method for simulating the mass transport process in porous media, Water Resour. Res., 35 (1999) 3649-3662.

[65] A.M. Tartakovsky, P. Meakin, T.D. Scheibe and R.M. Eichler West, Simulations of reactive transport and precipitation with smoothed particle hydrodynamics, J. Comput. Phys., 222 (2007) 654-672.

[66] A. Tompson and L. Gelhar, Numerical simulation of solute transport in three dimensional, randomly heterogeneous porous media, Water Resour. Res., 26 (1990) 2541-2562.

[67] C.F. Tsang and I. Neretnieks, Flow channeling in heterogeneous fractured rocks, Rev. Geophys., 36 (1998) 275-298.

[68] M. Tyagi, P. Jenny, I. Lunati and H-A. Tchelepi, A lagrangian, stochastic modeling framework for multi-phase flow in porous media, J. Comp. Phys., 227 (2008) 6696-6714.

[69] X.H. Wen and J.J. Gomez-Hernandez (1996), The constant displacement scheme for tracking particles in heterogeneous aquifers, Ground Water, 34 (1), 135-142.

[70] E.J. Wexler, Analytical solutions for one-, two-, and three-dimensional solute transport in ground-water systems with uniform flow : U.S. Geological Survey Techniques of Water-Resources Investigations, Book 3, Chapter B7, 1992.

[71] A. Younes and P. Ackerer, Solving the advection-diffusion equation with the Eulerian-Lagrangian localized adjoint method on unstructured meshes and non uniform time stepping, J. Comput. Phys., 208 (2005) 384-402.

[72] Z. Zhang and Q. Chen, Comparison of the Eulerian and Lagrangian methods for predicting particle transport in enclosed spaces, Atmos. Environ., 41 (2007) 5236-5248.

[73] C. Zheng nd G.D. Bennet, Applied contaminant transport modeling : second edition, John Wiley and Sons, New York, 2002.

[74] S. Zimmermann, P. Koumoutsakos and W. Zinzelbach, Simulation of pollutant transport using a particle method, J. Comput. Phys., 173 (2001) 322-347.

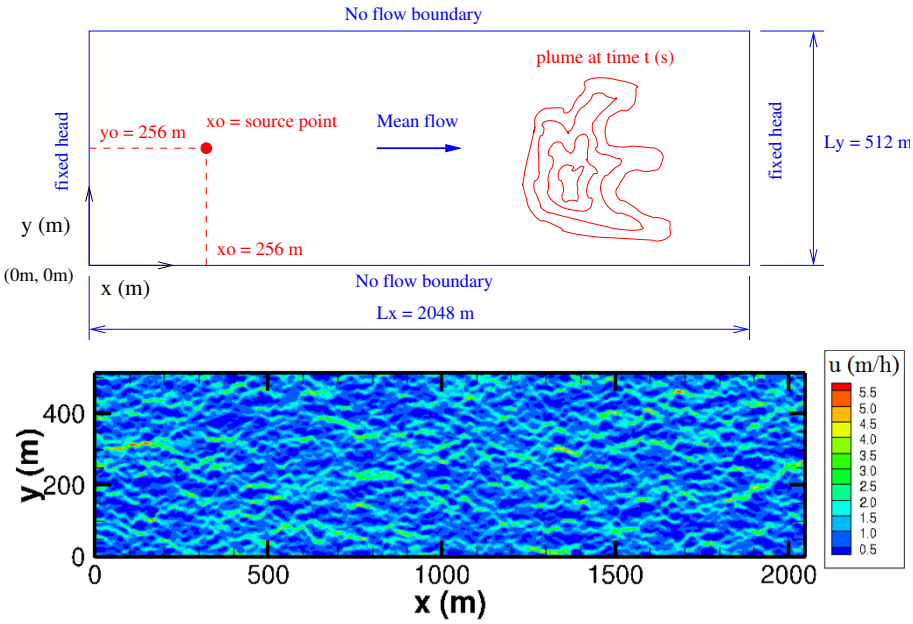

Figure 1: Top : sketch of benchmark 2, bottom : horizontal component of flow velocity.

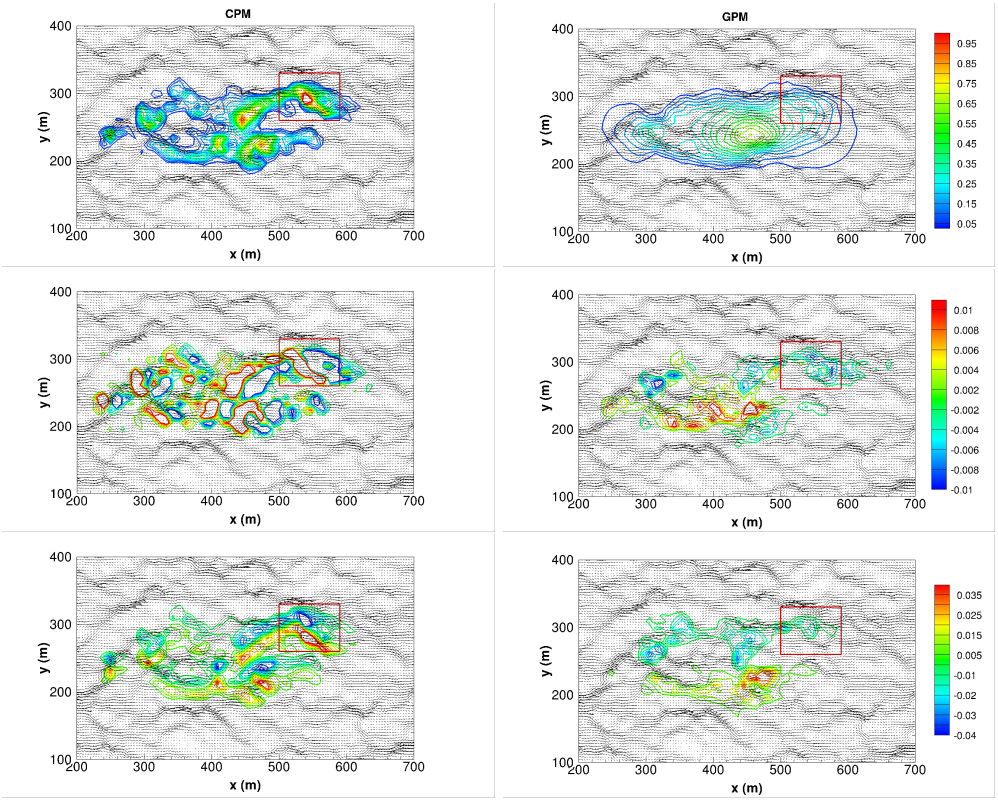

Figure 2: Difference of concentration δc (top), horizontal (middle) and vertical (bottom) components, g_x and g_y, of gradient $\mathbf{g}$ of concentration difference δc between the species A and B (colored contour lines) obtained by the concentration (left) and gradient (right) particle methods at time $t = 150\ h$ for a value of the grid cell size $h = 0.64\ m$ with a Peclet number $P_e = 100$. Arrows show the flow field.

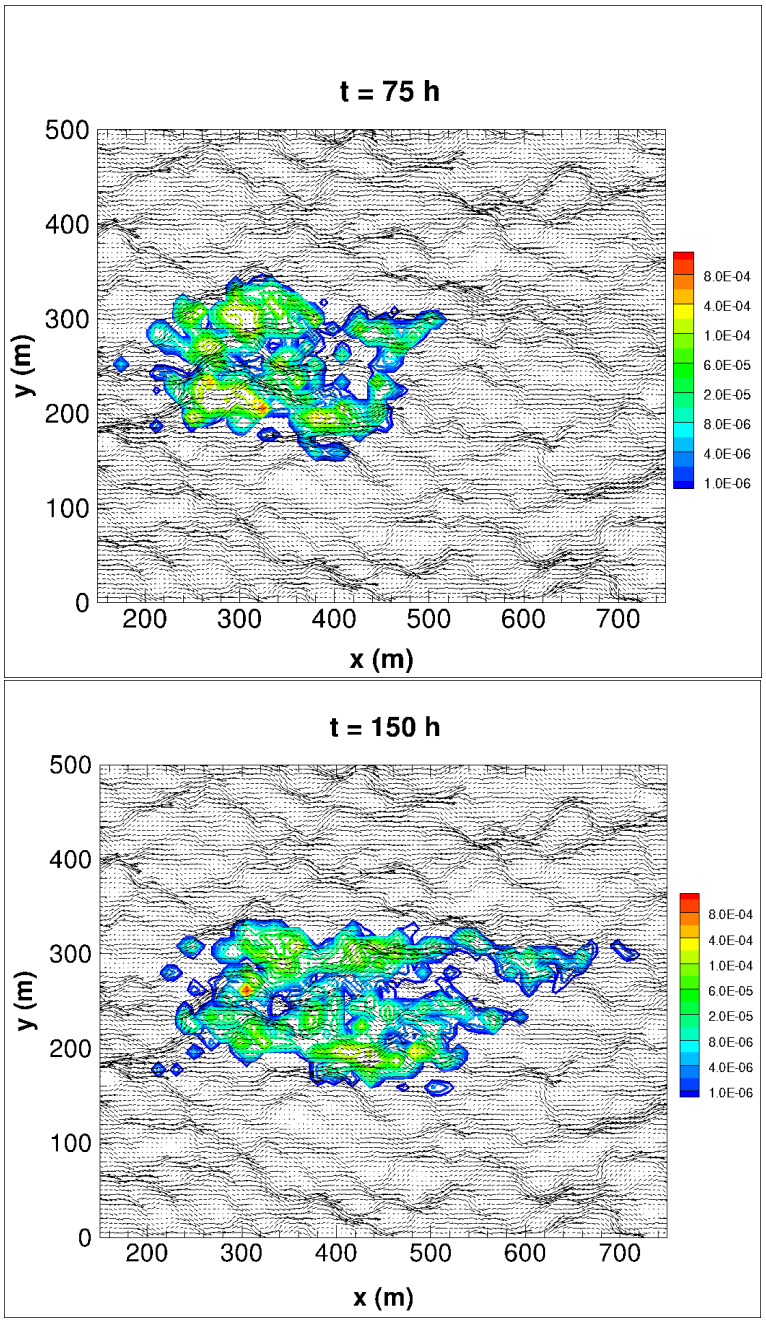

Figure 3: Reactive rate r (colored contour lines) obtained by the combined particle method at $t = 75\ h$ (top) and $150\ h$ (bottom) for a grid cell size $h = 0.64\ m$ with a Peclet number $P_e = 100$.

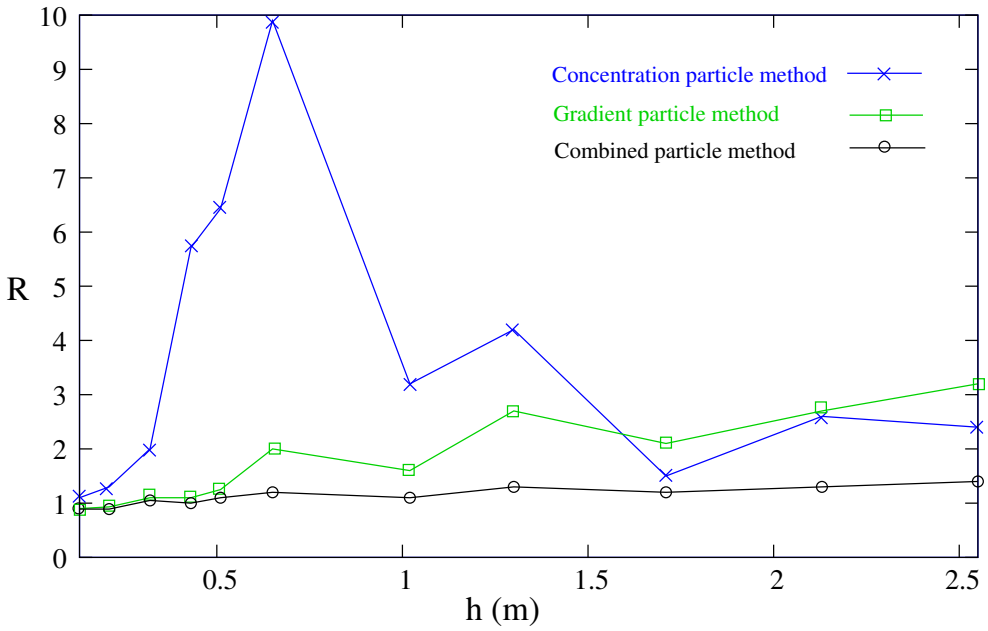

Figure 4: Integral R of the reactivity rate r over the computational domain as a function of the grid cell size h obtained by CPM (blue), GPM (green) and combined particle method (black) at time $t = 150\ h$ with a Peclet number $P_e = 100$.

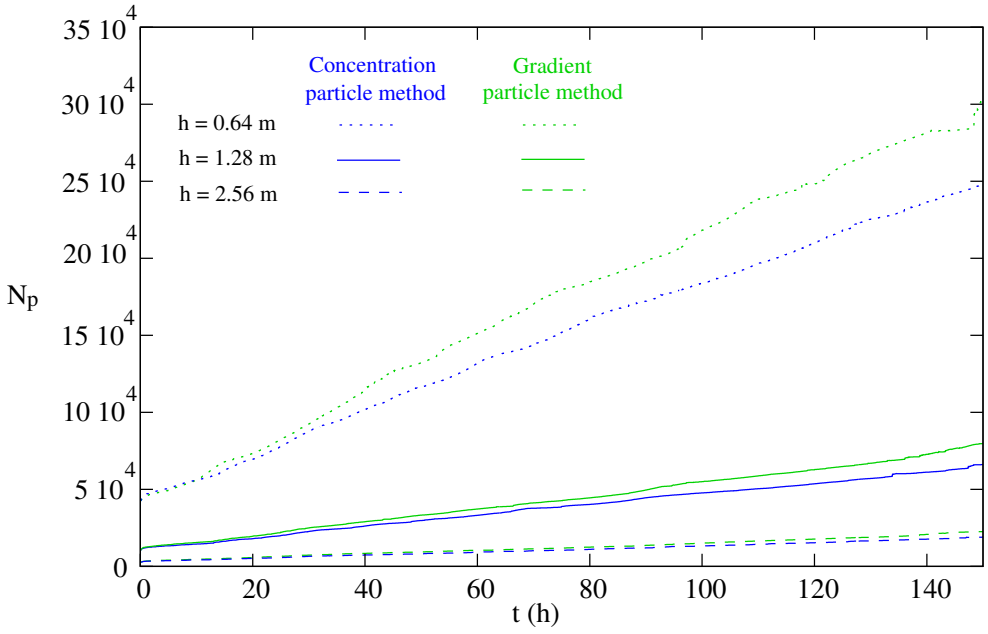

Figure 5: Time evolution of particle number N_p obtained by the concentration (blue) and gradient (green) particle methods for three values of the grid cell size $h = 0.64\ m$ (dotted line), $1.28\ m$ (solid line) and $2.56\ m$ (dashed line) with a Peclet number $P_e = 100$.

h (m)	N_{iter}	δt (h)	CPU time (h) with CPM	CPU time (h) with GPM
0.64	4688	0.032	11.56	12.87
1.28	2344	0.064	1.55	1.73
2.56	1172	0.128	0.24	0.27

Table 1: Iteration number N_{iter}, time step δt and CPU time for a physical time of 150 h obtained by the concentration (CPM) and gradient (GPM) particle methods with the three values of the grid cell size $h =$ 0.64, 1.28 and 2.56 m for a Peclet number $P_e = 100$. The numerical simulations were performed on a single processor Intel(R) Core(TM) i7-4800MQ CPU 2.70GHz.